Micromechanics of Spray-On Foam Insulation

Brett A. Bednarcyk* ‡ Senior Scientist

Jacob Aboudi* Professor

Steven M. Arnold† Research Engineer

Roy M. Sullivan† Research Engineer

Understanding the thermo-mechanical response of the Space Shuttle External Tank spray-on foam insulation (SOFI) material is critical to NASA's Return to Flight effort. This closed-cell rigid polymeric foam is used to insulate the metallic Space Shuttle External Tank, which is at cryogenic temperatures immediately prior to and during lift off. The shedding of the SOFI during ascent led to the loss of the Columbia, and eliminating/minimizing foam loss from the tank has become a priority for NASA as it seeks to resume scheduled space shuttle missions. Determining the nature of the SOFI material behavior in response to both thermal and mechanical loading plays an important role as any structural modeling of the shedding phenomenon is predicated on knowledge of the constitutive behavior of the foam.

In this paper, the SOFI material has been analyzed using the High-Fidelity Generalized Method of Cells (HFGMC) micromechanics model, which has recently been extended to admit a triply-periodic 3-D repeating unit cell (RUC). Additional theoretical extensions that were made in order to enable modeling of the closed-cell foam material include the ability to represent internal boundaries within the RUC (to simulated internal pores) and the ability to impose an internal pressure within the simulated pores. This latter extension is crucial as two sources contribute to significant internal pressure changes within the SOFI pores. First, gas trapped in the pores during the spray process will expand or contract due to temperature changes. Second, the pore pressure will increase due to outgassing of water and other species present in the foam skeleton polymer material. With HFGMC's new pore pressure modeling capabilities, a nonlinear pressure change within the simulated pore can be imposed that accounts for both of these sources, in addition to standard thermal and mechanical loading.

The triply-periodic HFGMC micromechanics model described above was implemented within NASA GRC's MAC/GMC software package, giving the model access to a range of nonlinear constitutive models for the polymeric foam skeleton material. A repeating unit cell architecture was constructed that, while relatively simple, still accounts for the geometric anisotropy of the porous foam microstructure and its thin walls and thicker edges. With the lack of reliable polymeric foam skeleton material properties, many simulations were executed aimed at backing out these material properties. Then, using these properties, predictions of the thermo-mechanical behavior of the foam, including calculated internal applied pressure profiles, were performed and compared with appropriate experimental data.

*Ohio Aerospace Institute, Ohio Aerospace Institute, NASA GRC, 21000 Brookpark Rd., Cleveland, USA 44135

†Mechanics and Lifing Branch, NASA Glenn Research Center, MS 49/7, 21000 Brookpark Rd., Cleveland, USA 44135

‡Corresponding Author; Contact Email: bednarcyk@oai.org

Micromechanics of Spray-On Foam Insulation

Brett A. Bednarcyk and Jacob Aboudi
Ohio Aerospace Institute, Cleveland, OH

Steven M. Arnold and Roy M. Sullivan
NASA Glenn Research Center, Cleveland, OH

Multi-Scale Approach to Modeling ET Foam Insulation

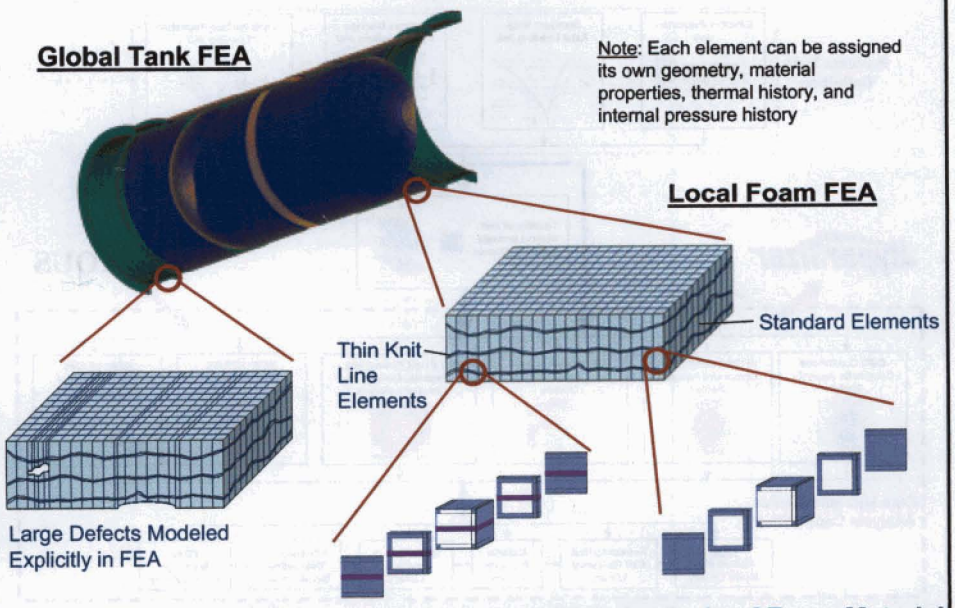

NASA/OAI ImMAC Software Suite for Multi-Scale Analysis of Advanced Materials & Structures

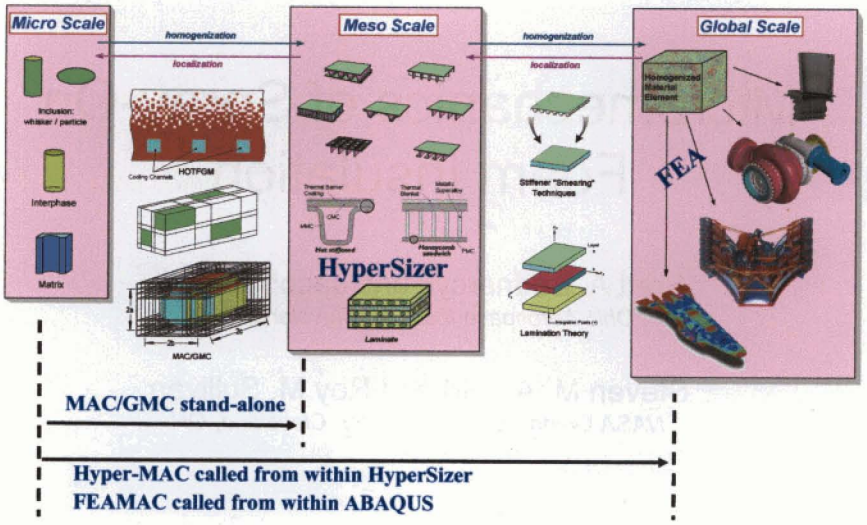

MAC/GMC Outline

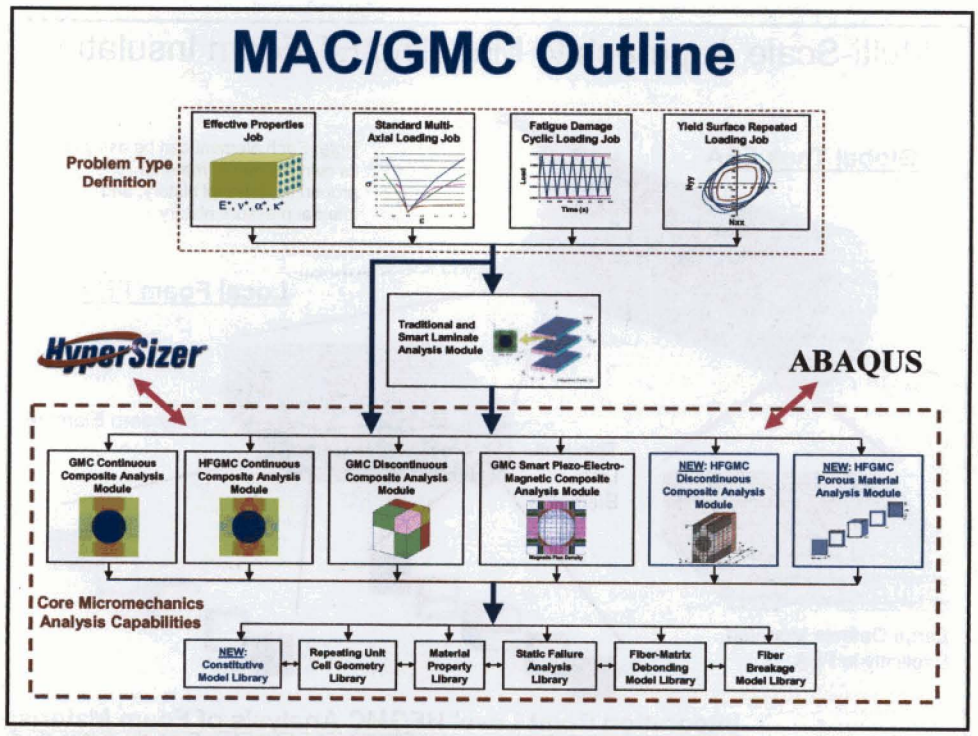

HFGMC Micromechanics Model: Geometry and Approach

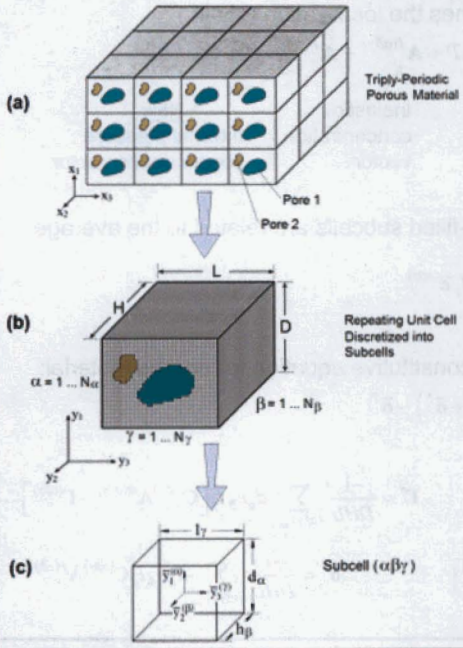

- HFGMC models a periodic *material*
- Repeating Unit Cell (RUC) is identified
- RUC is discretized into an arbitrary number of subcells ($\alpha\beta\gamma$)
- Subcells may contain any material, or be empty (pore)
- New capabilities included:

Internal Pore Pressure

Elastic Material Stiffening

Newtonian-Viscous Material Creep

HFGMC Micromechanics Model: Basic Equations

- Empty subcells subjected to internal pressure: $P^{(\alpha\beta\gamma)}$
- Constitutive equation within each subcell including inelastic and thermal strains:

$$\boldsymbol{\sigma}^{(\alpha\beta\gamma)} = \mathbf{C}^{(\alpha\beta\gamma)}\left(\boldsymbol{\varepsilon}^{(\alpha\beta\gamma)} - \boldsymbol{\varepsilon}^{I(\alpha\beta\gamma)}\right) - \boldsymbol{\Gamma}^{(\alpha\beta\gamma)}\Delta T$$

- Second-order displacement field assumed in each subcell:

$$\mathbf{u}^{(\alpha\beta\gamma)} = \bar{\boldsymbol{\varepsilon}}\,\mathbf{x} + \mathbf{W}_{(000)}^{(\alpha\beta\gamma)} + \bar{y}_1^{(\alpha)}\mathbf{W}_{(100)}^{(\alpha\beta\gamma)} + \bar{y}_2^{(\beta)}\mathbf{W}_{(010)}^{(\alpha\beta\gamma)} + \bar{y}_3^{(\gamma)}\mathbf{W}_{(001)}^{(\alpha\beta\gamma)} + \frac{1}{2}\left(3\bar{y}_1^{(\alpha)2} - \frac{d_\alpha^2}{4}\right)\mathbf{W}_{(200)}^{(\alpha\beta\gamma)}$$
$$+ \frac{1}{2}\left(3\bar{y}_2^{(\beta)2} - \frac{h_\beta^2}{4}\right)\mathbf{W}_{(020)}^{(\alpha\beta\gamma)} + \frac{1}{2}\left(3\bar{y}_3^{(\gamma)2} - \frac{l_\gamma^2}{4}\right)\mathbf{W}_{(002)}^{(\alpha\beta\gamma)}$$

- Unknown terms in each subcell, $\mathbf{W}_{lmn}^{(\alpha\beta\gamma)}$ determined via imposition of equilibrium, continuity, and periodicity equations in an average (integral) sense
- Results in system of linear algebraic equations for unknown terms: $\mathbf{KU} = \mathbf{f} + \mathbf{g}$
  - $\mathbf{K}$ - Contains geometry and thermo-mechanical property information
  - $\mathbf{U}$ - Contains unknown terms ($\mathbf{W}_{lmn}^{(\alpha\beta\gamma)}$)
  - $\mathbf{f}$ - Contains applied strain and temperature information
  - $\mathbf{g}$ - Contains integrals of inelastic strains and effects of system of pressures, $P^{(\alpha\beta\gamma)}$

HFGMC Micromechanics Model: Basic Equations

- Solving the system of equations establishes the localization relation:

$$\overline{\boldsymbol{\varepsilon}}^{(\alpha\beta\gamma)} = \mathbf{A}^{(\alpha\beta\gamma)}\overline{\boldsymbol{\varepsilon}} + \mathbf{A}^{th(\alpha\beta\gamma)}\Delta T + \mathbf{A}^{I(\alpha\beta\gamma)} + \mathbf{A}^{P(\alpha\beta\gamma)}$$

Mechanical concentration tensor — Thermal concentration vector — Inelastic concentration vector — New Internal pressure concentration vector

- The global average stress in the material-filled subcells are related to the average subcell stresses by:

$$\overline{\boldsymbol{\sigma}} = \frac{1}{DHL}\sum_{(\alpha\beta\gamma)_{filled}} d_\alpha h_\beta l_\gamma \overline{\boldsymbol{\sigma}}^{(\alpha\beta\gamma)}$$

- Above equations allow establishment of constitutive equation for porous material:

$$\overline{\boldsymbol{\sigma}} = \mathbf{C}^* \overline{\boldsymbol{\varepsilon}} - \left(\boldsymbol{\Gamma}^* \Delta T + \overline{\boldsymbol{\sigma}}^I\right) - \overline{\boldsymbol{\sigma}}^P$$

- Where,

$$\mathbf{C}^* = \frac{1}{DHL}\sum_{(\alpha\beta\gamma)_{filled}} d_\alpha h_\beta l_\gamma \mathbf{C}^{(\alpha\beta\gamma)}\mathbf{A}^{(\alpha\beta\gamma)} \qquad \boldsymbol{\Gamma}^* = \frac{-1}{DHL}\sum_{(\alpha\beta\gamma)_{filled}} d_\alpha h_\beta l_\gamma \left[\mathbf{C}^{(\alpha\beta\gamma)}\mathbf{A}^{th(\alpha\beta\gamma)} - \boldsymbol{\Gamma}^{(\alpha\beta\gamma)}\right]$$

$$\overline{\boldsymbol{\sigma}}^I = \frac{-1}{DHL}\sum_{(\alpha\beta\gamma)_{filled}} d_\alpha h_\beta l_\gamma \left[\mathbf{C}^{(\alpha\beta\gamma)}\mathbf{A}^{I(\alpha\beta\gamma)} - \mathbf{R}^{(\alpha\beta\gamma)}_{(0,0,0)}\right] \qquad \overline{\boldsymbol{\sigma}}^P = \frac{-1}{DHL}\sum_{(\alpha\beta\gamma)_{filled}} d_\alpha h_\beta l_\gamma \mathbf{C}^{(\alpha\beta\gamma)}\mathbf{A}^{P(\alpha\beta\gamma)}$$

Modeling Smooth Tensile Test Specimen Results

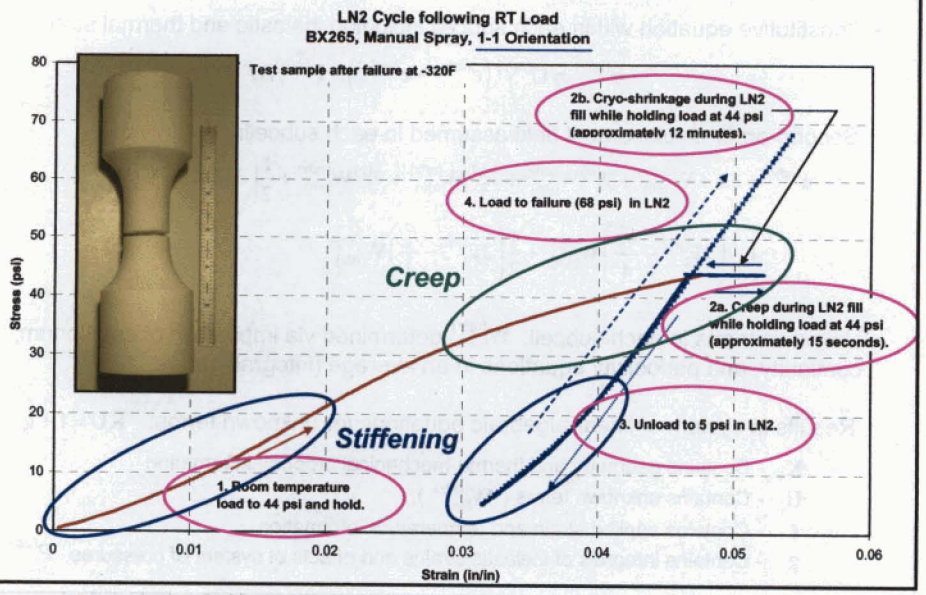

Implementing Stiffening and Creep

- Models need to be relatively simple, but capture primary effects
- Elastic Stiffening Constitutive Model (Chen and Saleeb, 1981):
  - Bulk Modulus: $K(\varepsilon_v) = K_0 + K_1\varepsilon_v + K_2\varepsilon_v^2$

    volumetric strain: $\varepsilon_v = \varepsilon_{11} + \varepsilon_{22} + \varepsilon_{33}$
  - Shear Modulus: $G\left(p, \sqrt{J_2}\right) = G_0 + A_1 p + A_2\sqrt{J_2}$

    $J_2 = \frac{1}{2} S_{ij} S_{ij}$ $\qquad p = \frac{1}{3}(\sigma_{11} + \sigma_{22} + \sigma_{33})$
  - For simplicity reduce to two parameters, set: $K_2 = A_1 = 0$
- Newtonian-Viscous Creep Model for Polymers (Ashby and Jones, 1980):

$\dot{\varepsilon}_{creep} = A\sigma e^{-Q/RT}$ $\qquad Q$ = Creep activation energy

A = Creep coefficient

Creep and Stiffening Model for Skeleton Material

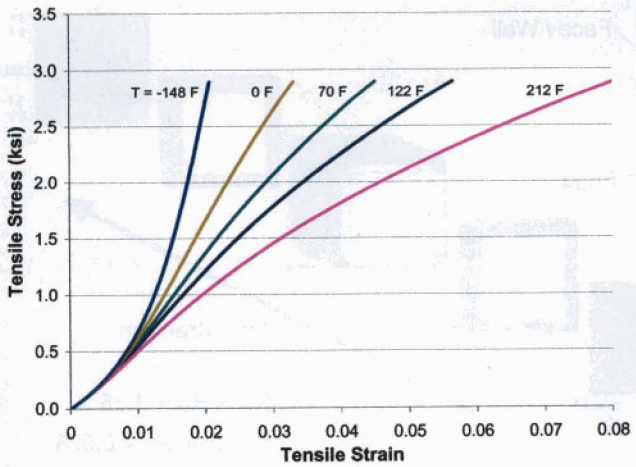

Notes

- Only tensile ε_v causes stiffening
- Creep strain does not contribute to stiffening
- Creep highly dependent on time/loading rate
- Temp-dependence of creep automatic through Arrhenius eq.
- Additional temp-dependence of G_0 and K_0 not shown in chart

Model Variables

- Geometry
  - Aspect Ratio
  - Wall Thickness
  - Edge Thickness
  - Unit Cell Discretization

  } Treat as fixed

- Material Properties
  - Elastic: $E_0(T)$, $\nu_0 = 0.4$
  - Elastic Stiffening: K_1, A_2
  - Creep: A, Q
  - Thermal Expansion: $\alpha(T)$

  } Attempt to determine to achieve good agreement

Geometry – BX 265

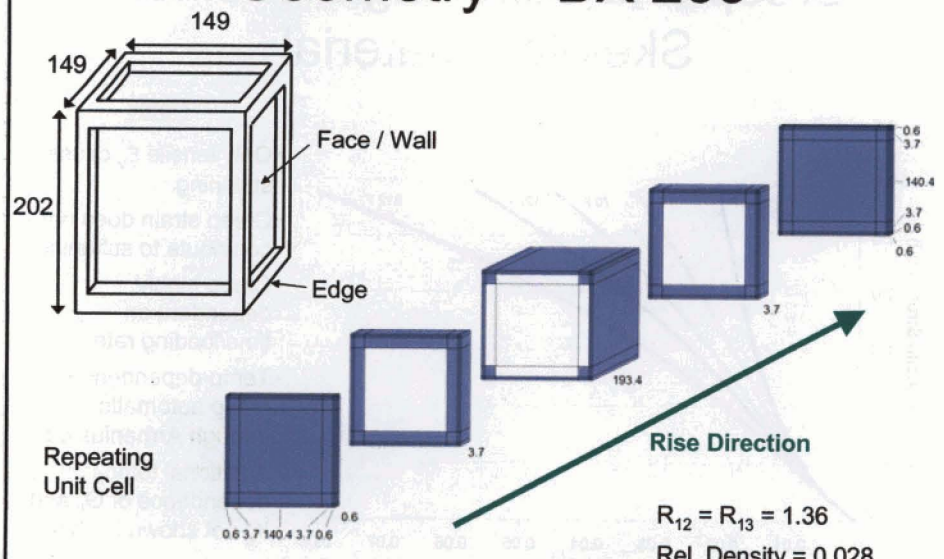

$R_{12} = R_{13} = 1.36$

Rel. Density = 0.028

(Bx-265 Auto Low data provided by B. Lerch, NASA GRC)

Room Temp Loading and 15 s Creep

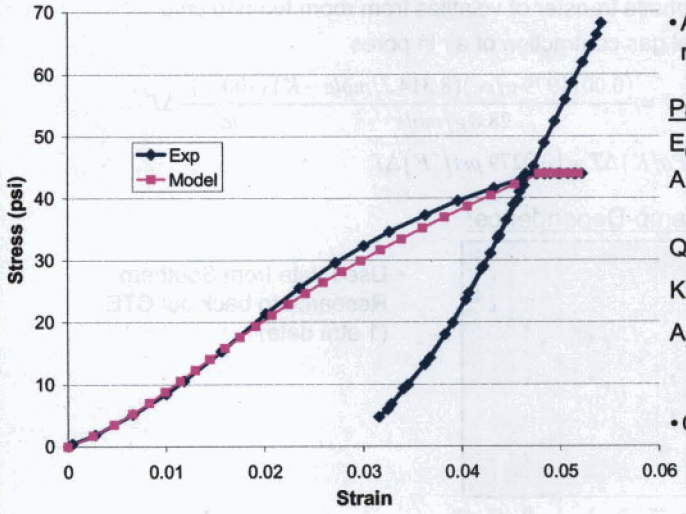

Note

- Assumed same loading rate as notched test

Parameters characterized

E_0 = 270 MPa (39 ksi)

A = 0.00104 MPa^{-1} s^{-1} (0.00715 ksi^{-1} s^{-1})

Q = 10,000 J/mole

K_1 = 7500 MPa (1088 ksi)

A_2 = 30

Next Step

- Cool Down to -320 F

Cool Down to -320 F

- Interaction of many effects:
  - E_0 temp-dependence
  - Pore pressure change
  - CTE and CTE temp-dependence
  - Creep: temp-dependence due to Arrhenius term
    - Temp. change rate (significantly affects creep)
- E_0 temp-dependence:

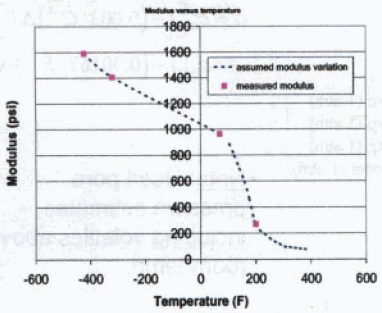

- Utilized E vs. T data
- -320 F vs. 68 F → E increase by 46%
- Assume linear increase in skeleton material E_0 from room temp to cryo

$$E = E_0\left[1-\left(0.002115\ ^\circ C^{-1}\right)\Delta T\right]$$
$$= E_0\left[1-\left(0.001175\ ^\circ F^{-1}\right)\Delta T\right]$$

Cool Down to -320 F

- Pore pressure change:
  - Assume no phase transfer of volatiles from room temp to cryo
  - Assume ideal gas contraction of air in pores

$$\Delta P_{air} = \frac{\rho_{air} R}{M_{air}} \Delta T = \frac{(0.0011979\, g/cc)(8.314\, J/mole-K)}{28.8\, g/mole} \frac{(100cc)^3}{m^3} \Delta T$$
$$= (345.8\, Pa/K)\Delta T = (0.0279\, psi/^\circ F)\Delta T$$

- CTE and CTE Temp-Dependence:

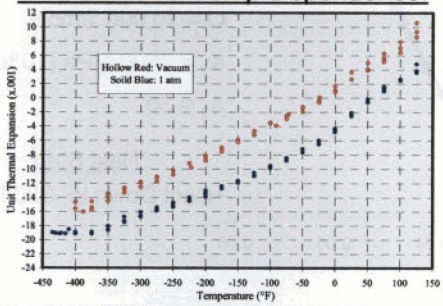

Figure 1. Comparison Thermal Expansion of BX 265 (3") in the 11 direction under Vacuum and at 1 atm. & 0.9 psi load

- Used data from Southern Research to back out CTE (1 atm data)

CTE and CTE Temp-Dependence

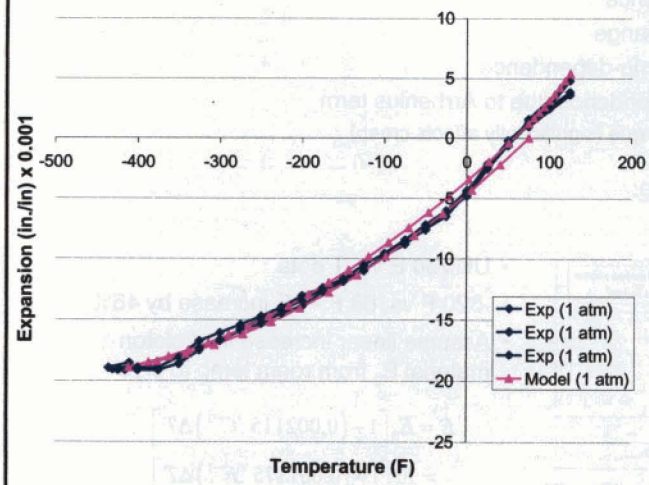

- Assumed linear CTE temp-dependence
- $\alpha(T = 70\ F) = \alpha_0 = 120 \times 10^{-6}/C\ (67 \times 10^{-6}/F)$

$$\alpha = \alpha_0\left[1-(0.003\ ^\circ C^{-1})\Delta T\right]$$
$$= \alpha_0\left[1-(0.00167\ ^\circ F^{-1})\Delta T\right]$$

- Note: Used pore pressure estimates including volatiles above room temp

Prediction of Southern Research Vacuum Data

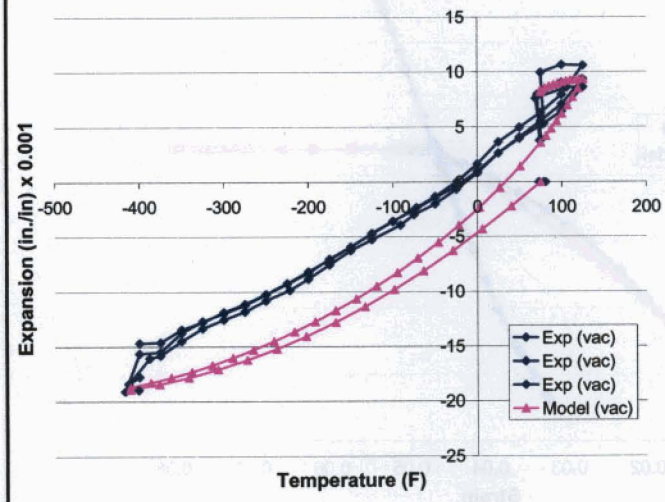

Test Sequence

- Cool to cryo at 1atm
- Pull vacuum
- Heat to 125 F
- Cool to 75
- Release vacuum

Model Sequence

point	Time (s)	Temp (F)	Pext (psi)	Pint (psi)
1	0	75	14.7	0.00
2	1400	-410	14.7	-13.51
3	1900	-410	0	1.19
4	9200	75	0	14.70
5	10000	125	0	23.18
6	11000	75	0	14.70
7	11120	75	14.7	0.00

Cool Down to -320 F

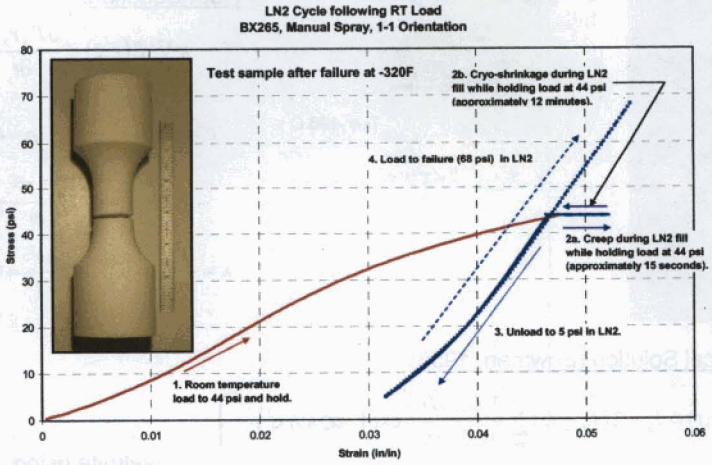

- Last item needed is cool down rate (temperature vs. time)
- First tried linear temp. vs. time

Cool Down to -320 F

(assuming linear time vs. temp.)

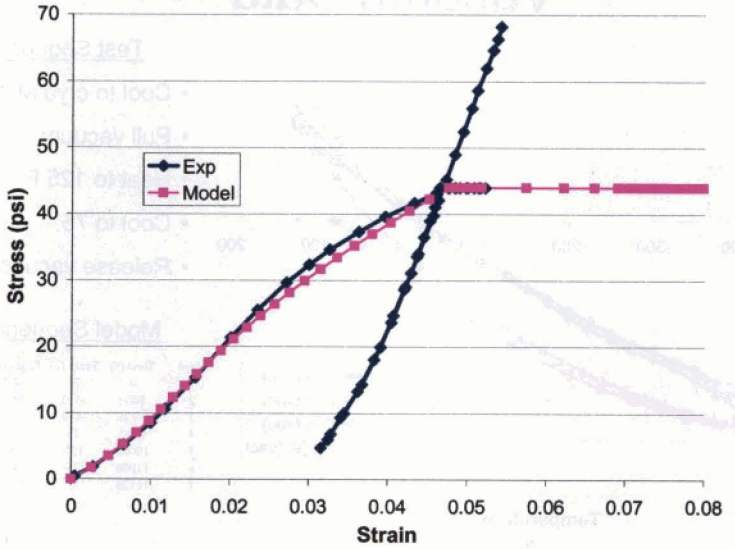

Transient Heat Transfer in Cylinder

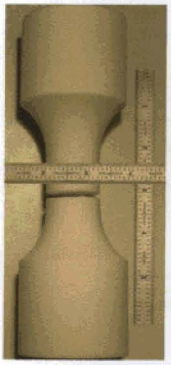

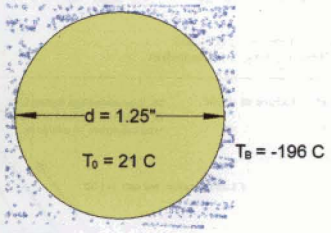

Heat Equation:

$$\kappa \nabla^2 T(r,t) = \frac{\partial T(r,t)}{\partial t}$$

$$c = 1065 \frac{J}{kg\ ^\circ C} \qquad \rho = 41.5 \frac{kg}{m^3}$$

$$k = 0.0293 \frac{W}{m\ ^\circ C}$$

$$\kappa = \frac{k}{c\rho} = 6.62 \times 10^{-7} \frac{m^2}{s} = 0.00103 \frac{in^2}{s}$$

Analytical Solution (Bowman, 1958)

$$T(r,t) = T_B - 2(T_B - T_0) \sum_{n=1}^{\infty} \frac{J_0(\alpha_n r/r_0)}{\alpha_n J_1(\alpha_n)} \exp\left(-\alpha_n^2 \kappa t / r_0^2\right)$$

J_0, J_1 Bessel functions of the 1st kind

α_n nth positive zero of J_0

Evaluate using Mathematica

Transient Heat Transfer in Cylinder

- Also performed ABAQUS FEA heat transfer analyses:

DC3D8 Brick

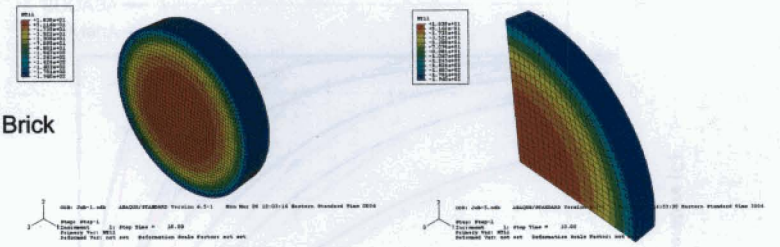

DC3D6 Wedge

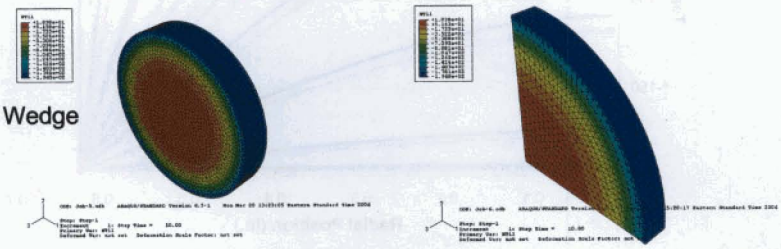

Transient Heat Transfer in Cylinder

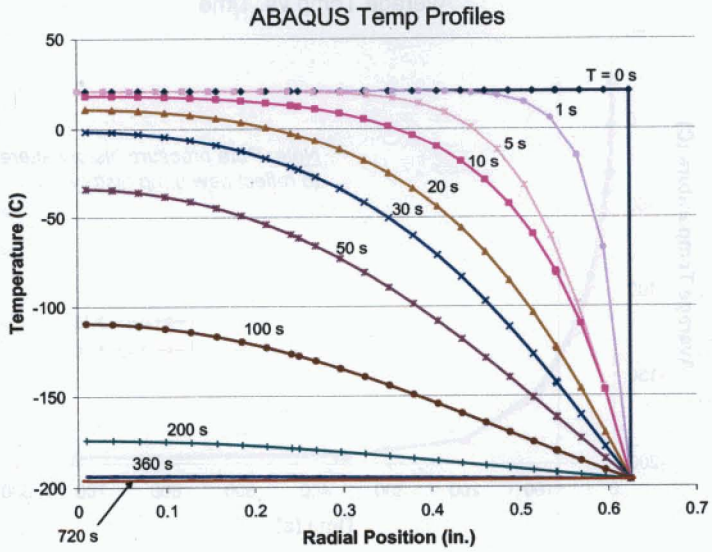

Transient Heat Transfer in Cylinder

ABAQUS Temp Profiles vs. Analytical Temp Profiles

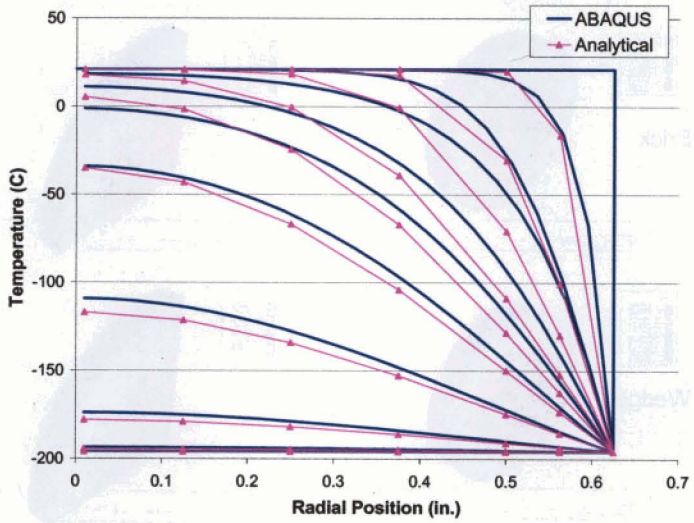

Transient Heat Transfer in Cylinder

Average Temp vs. Time

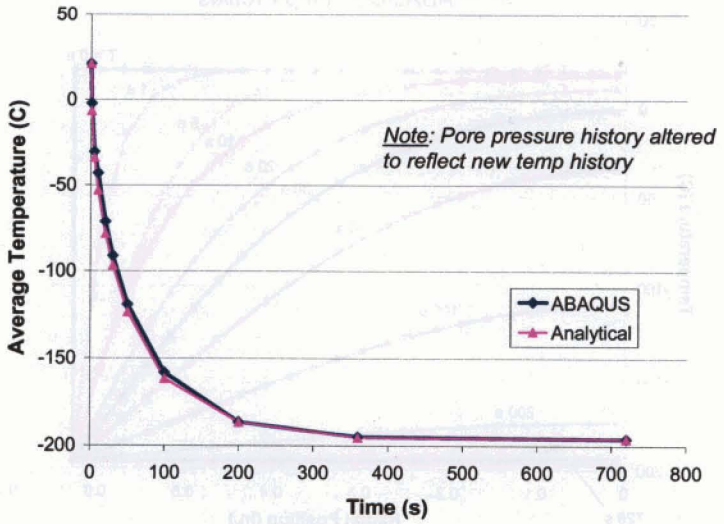

Cool Down to -320 F

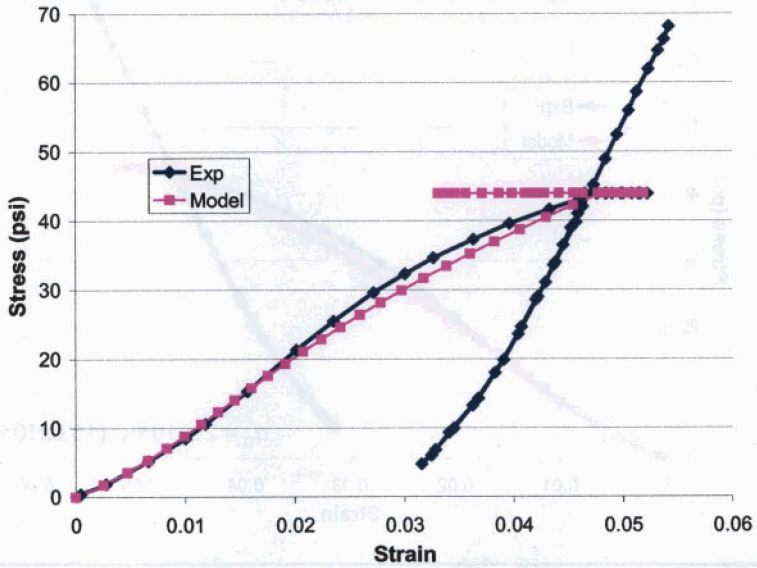

Cool Down to -320 F Inconsistent with Southern Research Data

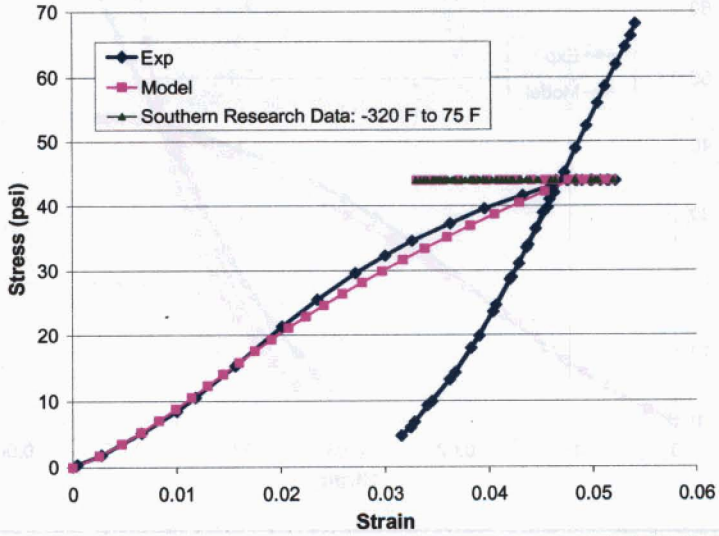

Re-calibrate CTE

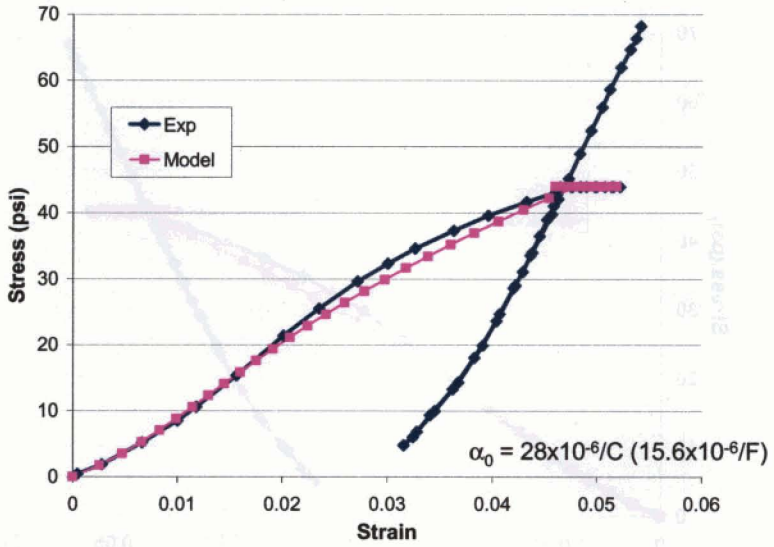

Full Smooth Tensile Test Simulation

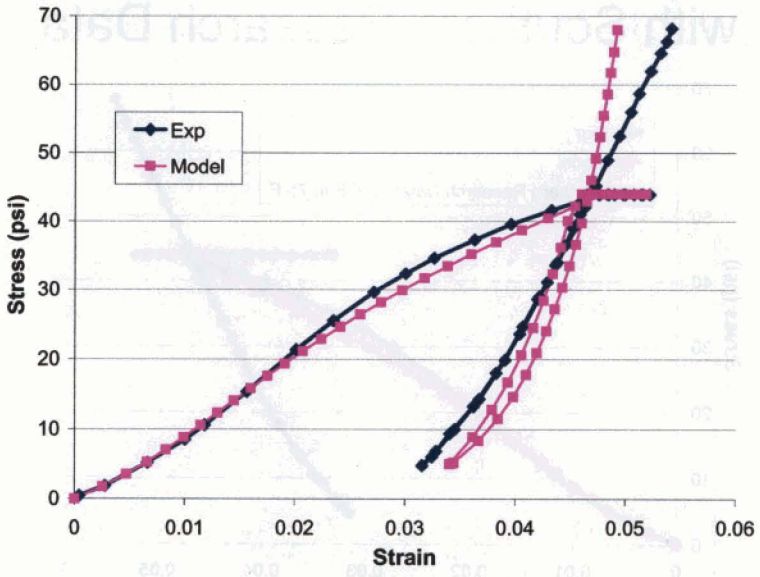

GRC Thermal Expansion Data (Feb. 2006)

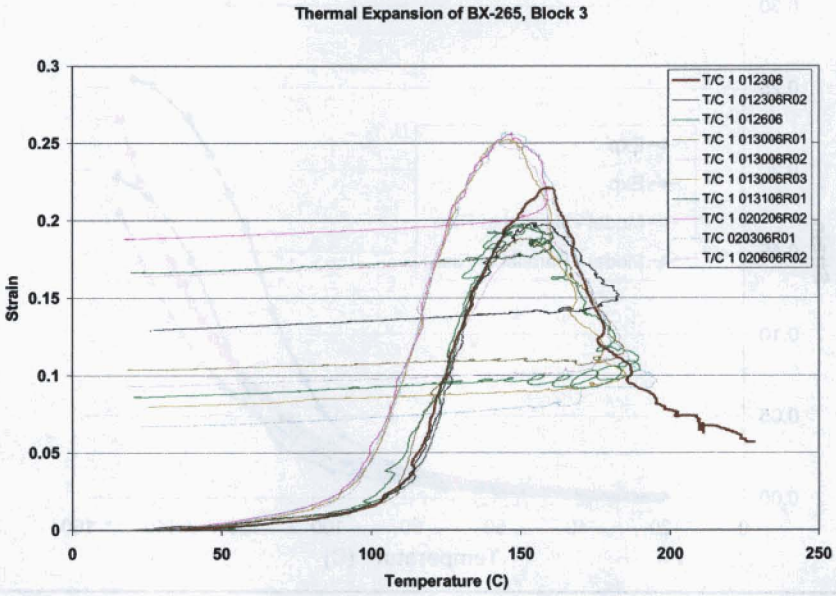

Elevated Temperature Pore Pressure Estimates

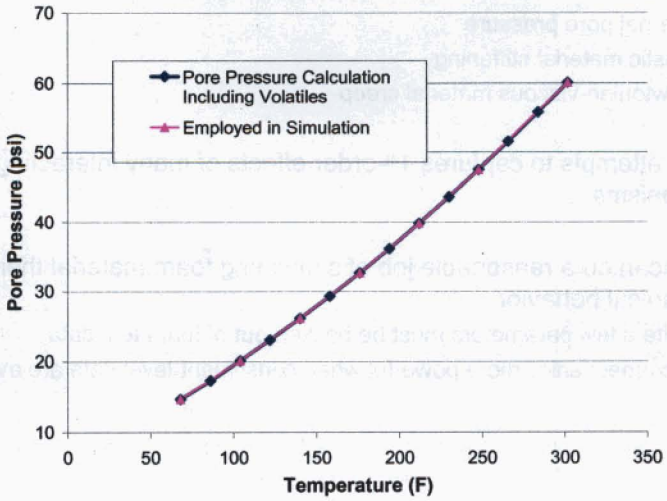

GRC Thermal Expansion Test Simulation

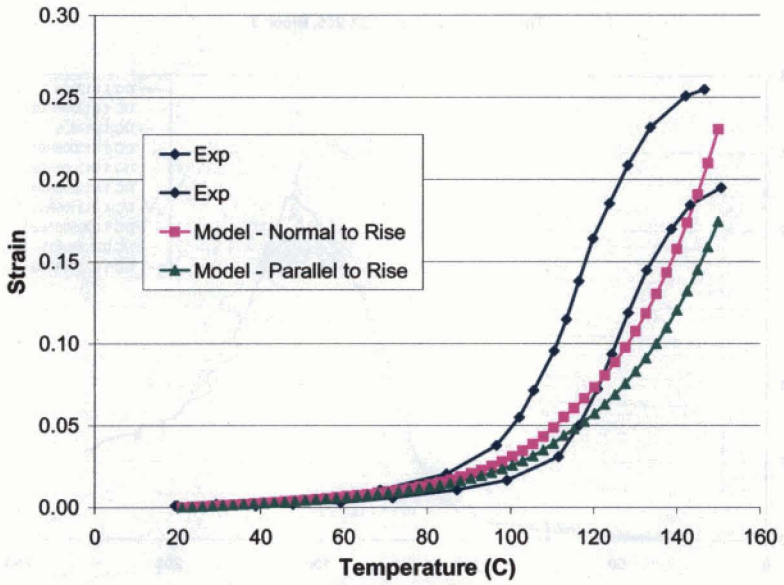

Conclusion

- NASA/OAI ImMAC suite enhanced to enable micromechanics analysis of foams with:
  - Internal pore pressure
  - Elastic material stiffening
  - Newtonian-viscous material creep
- Model attempts to captures 1st-order effects of many interacting mechanisms
- Model can do a reasonable job of simulating foam material thermo-mechanical behavior
  - Quite a few parameters must be backed out of foam test data
  - Micromechanics more powerful when constituent-level data are available